

Investigation of Surface Structures by Powder Diffraction: A Differential Pair Distribution Function Study on Arsenate Sorption on Ferrihydrite

Richard Harrington,^{*,†,||} Douglas B. Hausner,[‡] Narayan Bhandari,[‡] Daniel R. Strongin,[‡] Karena W. Chapman,[§] Peter J. Chupas,[§] Derek S. Middlemiss,^{||} Clare P. Grey,^{||} and John B. Parise^{†,||}

[†]Department of Geosciences, Stony Brook University, Stony Brook, New York 11794, [‡]Department of Chemistry, Temple University, Philadelphia, Pennsylvania 19122, [§]X-ray Science Division, Argonne National Laboratory, Advanced Photon Source, Argonne, Illinois 60439, and ^{||}Department of Chemistry, Stony Brook University, Stony Brook, New York 11794

Received November 16, 2009

Differential pair distribution function (d-PDF) analysis of high energy powder X-ray diffraction data was carried out on 2-line ferrihydrite nanoparticles with arsenate oxyanions adsorbed on the surface to investigate the binding mechanism. In this analysis, a PDF of ferrihydrite is subtracted from a PDF of ferrihydrite with arsenate sorbed on the surface, leaving only correlations from within the surface layer and between the surface and the particle. As–O and As–Fe correlations were observed at 1.68 and 3.29 Å, respectively, in good agreement with previously published EXAFS data, confirming a bidentate binuclear binding mechanism. Further peaks are observed in the d-PDF which are not present in EXAFS, corresponding to correlations between As and O in the particle and As–2nd Fe.

Introduction

X-ray diffraction has been widely used for a century or so to determine the relative position of atoms in solids. Routinely, crystal structures are determined by examination of the Bragg peaks diffracted from a single crystal with dimensions of tens of micro meters or more. In the past few decades, the improvement in powder diffraction instrumentation and development of Rietveld refinement techniques has permitted the refinement of crystal structures from polycrystalline samples, multigrain samples with grain sizes of the order of a micro meter, to become commonplace. Both techniques scrutinize the positions and intensities of Bragg peaks, arising as a consequence of long-range order in the sample.

More recently, with the advent of high energy synchrotron and spallation neutron sources, pair distribution function (PDF) analysis of powder diffraction data has been applied to crystalline materials.^{1–3} PDF analysis involves taking the Fourier transform of the total structure function (both the Bragg and diffuse scattering), yielding a real space distribution of distances between pairs of atoms in a structure weighted by the scattering power of the atoms responsible for the peak. The technique has proved powerful in solids

where the local structure differs from the average structure.^{4–6} High values of the elastic scattering vector, $Q = 4\pi \sin \theta / \lambda$, are required as the real space resolution is directly related to the value of Q_{\max} used in the Fourier transform. Since PDF analysis does not rely upon the presence of periodicity in a sample, it has proved to be a useful tool in studies of nanomaterials, that is, materials composed of particles less than 100 nanometers.^{7–10}

The PDF method is highly complementary to extended X-ray absorption fine structure (EXAFS); both methodologies provide local structural information on bond lengths and coordination numbers. There are, however, a few notable differences between the two experimental approaches. While the PDF technique is not prone to phase shift and Debye–Waller anomalies, as is common in EXAFS analyses, it is also not intrinsically element or chemical specific. Peaks present in the PDF correspond to correlations between all pairs of atoms within the sample, not limited to the first few coordination shells. Although this permits for the investigation of a greater number of atomic correlations in the structure, it can also lead to considerable overlap of peaks corresponding to

*To whom correspondence should be addressed. E-mail: richard.harrington@stonybrook.edu.

(1) Billinge, S. J. L.; Kanatzidis, M. G. *Chem. Commun.* **2004**, 749–760.
(2) Egami, T.; Billinge, S. J. L. *Underneath the Bragg peaks: Structural analysis of complex materials*; Oxford: New York, 2003.
(3) Proffen, T.; Kim, H. J. *Mater. Chem.* **2009**, *19*, 5078–5088.
(4) Jeong, I.-K.; Mohiuddin-Jacobs, F.; Petkov, V.; Billinge, S. J. L.; Kycia, S. *Phys. Rev. B* **2001**, *63*, 205202.

(5) Kim, Y. I.; Page, K.; Limarga, A. M.; Clarke, D. R.; Seshadri, R. *Phys. Rev. B* **2007**, *76*, 115204.
(6) Laulhe, C.; Hippert, F.; Bellissent, R.; Simon, A.; Cuello, G. J. *Phys. Rev. B* **2009**, *79*, 064104.
(7) Gilbert, B.; Huang, F.; Zhang, H.; Waychunas, G. A.; Banfield, J. F. *Science* **2004**, *305*, 651–654.
(8) Michel, F. M.; Antao, S. M.; Chupas, P. J.; Lee, P. L.; Parise, J. B.; Schoonen, M. A. A. *Chem. Mater.* **2005**, *17*, 6246–6255.
(9) Waychunas, G. A.; Zhang, H. *Elements* **2008**, *4*, 381–387.
(10) Petkov, V. *Mater. Today* **2008**, *11*(11), 28–38.

multiple correlations of similar length, often complicating subsequent analyses.

In this contribution, we present a study of the adsorbate structure of surface species on nanoparticles using differential pair distribution function (d-PDF) analysis of total X-ray scattering data.^{11–13} In a d-PDF experiment, a reference pattern from the unloaded nanoparticles is subtracted from a pattern arising from a “host + guest” sample, so as to isolate only the correlations involving the sorbed species: the guest–guest and guest–host interactions. This method offers the potential to mitigate some of the difficulties posed by the analysis of conventional PDF experiments, as outlined above. An example of the use of this technique may be found in the study of Chapman et al. that investigated the bonding mechanism of gas molecules (hydrogen and nitrogen) within the pores of the Prussian Blue analogue $\text{Mn}^{\text{II}}_3[\text{Co}^{\text{III}}(\text{CN})_6]_2$, d-PDF analyses being applied to both X-ray and neutron powder diffraction data.^{14,15} In the later work, the unloaded Prussian Blue constituted the blank, while the sample comprised the same powder under a steady flow of hydrogen gas. d-PDF analysis revealed that the H_2 molecule adsorbs at the center of a pore, rather than binding to the Mn^{II} ion. Sensitivities down to 1 wt % have been demonstrated.¹⁵ The approach to d-PDF analysis outlined above and used in the present work makes more direct contact with local chemical concepts such as bonding and coordination and differs substantially from techniques exploiting the contrast afforded by anomalous scattering or neutron isotope effects, which are also sometimes referred to as differential PDF.¹⁶

The present study examines the adsorption of arsenic(V) oxyanions on the surface of 2-line ferrihydrite (named for the number of broad peaks in its X-ray diffraction pattern), a naturally occurring iron oxyhydroxide nanoparticle.^{17–19} Ferrihydrite, ubiquitous in many natural systems, is extremely effective in the sequestration of many transition metals and metalloids.^{20–22} Industrial chemists utilize ferrihydrite to scavenge trace elements, such as arsenic, in the treatment of

wastewaters²³ and in processing activities such as direct coal liquefaction and metallurgy.²⁴

The mechanism of arsenate adsorption on the surface of these nanoparticles has significant relevance to the means by which these trace elements might be removed from water and in understanding their transport behavior.^{25–29} Previous studies show that arsenate(V) oxyanions sorb strongly to the surface of ferrihydrite.^{26,30–32} Waychunas et al.,³³ using EXAFS, showed that the arsenate ion adsorbs on ferrihydrite as an inner-sphere complex, that is bound directly to the surface rather than through a separating water layer, this latter mechanism being termed outer sphere complexation; although there is some evidence that outer sphere coordination exists along with inner sphere.³⁴ Waychunas et al.³³ proposed that the AsO_4 tetrahedron binds to the surface in a bidentate binuclear geometry in which the tetrahedron links through two oxygen atoms to two distinct iron sites. After some debate in the literature,^{35,36} this binding geometry was confirmed by Sherman and Randall³⁷ using a combination of density functional theory (DFT) calculations and EXAFS spectroscopy experiments.

In this study, d-PDF analyses are applied to further investigate the conclusions reached by Sherman and Randall³⁷ and to examine whether any further insights are made available by this technique.

Experimental Methods

Two-line ferrihydrite was synthesized at room temperature by adding 1 M NaOH to a 0.1 M solution of FeCl_3 with constant stirring until pH 7.5 was reached. The colloidal suspension was then dialyzed to remove counterions. For d-PDF measurements, the suspension was separated into five aliquots. The aliquots were centrifuged down, decanted, and individually mixed with solutions having sodium arsenate concentrations of 100 mM, 10 mM, 1 mM, or 0.1 mM. Ferrihydrite exposed to deionized water served as a control sample. The suspensions were allowed to equilibrate for 1 h, then centrifuged and rinsed once with deionized water. Finally, the exposed and washed suspensions were allowed to air-dry.

Transmission electron microscopy (TEM) bright field micrographs were collected using a Tecnai 12 T TEM operating at 120 kV housed at the Microanalysis and Imaging Research and Training Center at West Chester University. Arsenate exposed samples were analyzed to confirm that there were no

(11) Petkov, V.; Billinge, S. J. L.; Vogt, T.; Ichimura, A. S.; Dye, J. L. *Phys. Rev. Lett.* **2002**, *89*(7), 075502.

(12) Billinge, S. J. L.; McKimmy, E. J.; Shatnawi, M.; Kim, H.; Petkov, V.; Wermeille, D.; Pinnavaia, T. J. *J. Am. Chem. Soc.* **2005**, *127*, 8492–8498.

(13) Chupas, P. J.; Chapman, K. W.; Jennings, G.; Lee, P. L.; Grey, C. P. *J. Am. Chem. Soc.* **2007**, *129*(45), 13822–13824.

(14) Chapman, K. W.; Chupas, P. J.; Kepert, C. J. *J. Am. Chem. Soc.* **2005**, *127*(32), 11232–11233.

(15) Chapman, K. W.; Chupas, P. J.; Maxey, E. R.; Richardson, J. W. *Chem. Commun.* **2006**, No. 38, 4013–4015.

(16) Petkov, V.; Jeong, I.-K.; Mohiuddin-Jacobs, F.; Proffen, T.; Billinge, S. J. L.; Dmowski, W. *J. Appl. Phys.* **2000**, *88*(2), 665–672.

(17) Jambor, J. L.; Dutrizac, J. E. *Chem. Rev.* **1998**, *98*, 2549–2585.

(18) Michel, F. M.; Ehm, L.; Antao, S. M.; Lee, P. L.; Chupas, P. J.; Li, G.; Strongin, D. R.; Schoonen, M. A. A.; Phillips, B. L.; Parise, J. B. *Science* **2006**, *316*, 1726–1729.

(19) Michel, F. M.; Ehm, L.; Liu, G.; Han, W. Q.; Antao, S. M.; Chupas, P. J.; Lee, P. L.; Knorr, K.; Eulert, H.; Kim, J.; Grey, C. P.; Celestian, A. J.; Gillow, J.; Schoonen, M. A. A.; Strongin, D. R.; Parise, J. B. *Chem. Mater.* **2007**, *19*, 1489–1496.

(20) Sadiq, M. *Water, Air, Soil Pollut.* **1997**, *93*(1–4), 117–136.

(21) Welch, A. H.; Westjohn, D. B.; Helsel, D. R.; Wanty, R. B. *Ground Water* **2000**, *38*(4), 589–604.

(22) Waychunas, G. A.; Kim, C. S.; Banfield, J. F. *J. Nanopart. Res.* **2005**, *7*, 409–433.

(23) Streat, M.; Hellgardt, K.; Newton, N. R. L. *Process Saf. Environ. Prot.* **2008**, *86*, 11–20.

(24) Huffman, G. P.; Ganguly, B.; Zhao, J.; Rao, K. R. P. M.; Shah, N.; Feng, Z.; Huggins, F. E.; Taghiei, M. M.; Lu, F.; Wender, I.; Pradhan, V. R.; Tierney, J. W.; Seehra, M. S.; Ibrahim, M. M.; Shabtai, J.; Eyring, E. M. *Energy Fuels* **1993**, *7*, 285–296.

(25) Goldberg, S.; Johnston, C. T. *J. Colloid Interface Sci.* **2001**, *234*, 204–216.

(26) Raven, K. P.; Jain, A.; Loeppert, R. H. *Environ. Sci. Technol.* **1998**, *32*, 344–349.

(27) Dixit, S.; Hering, J. G. *Environ. Sci. Technol.* **2003**, *37*, 4182–4189.

(28) Wang, S.; Mulligan, C. N. *Environ. Int.* **2008**, *34*, 867–879.

(29) Kubicki, J. D.; Kwon, K. D.; Paul, K. W.; Sparks, D. L. *Eur. J. Soil Sci.* **2007**, *58*, 932–944.

(30) Fuller, C. C.; Davis, J. A.; Waychunas, G. A. *Geochim. Cosmochim. Acta* **1993**, *57*, 2271–2282.

(31) Jain, A.; Raven, K. P.; Loeppert, R. H. *Environ. Sci. Technol.* **1999**, *33*(8), 1179–1184.

(32) Roddick-Lanzilotta, A. J.; McQuillan, A. J.; Craw, D. *Appl. Geochem.* **2002**, *17*, 445–454.

(33) Waychunas, G. A.; Rea, B. A.; Fuller, C. C.; Davis, J. A. *Geochim. Cosmochim. Acta* **1993**, *57*, 2251–2269.

(34) Carabante, I.; Grahn, M.; Holmgren, A.; Kumpieni, J.; Hedlund, J. *Colloids Surf., A* **2009**, *346*, 106–113.

(35) Manceau, A. *Geochim. Cosmochim. Acta* **1995**, *59*(17), 3647–3653.

(36) Waychunas, G. A.; Davis, J. A.; Fuller, C. C. *Geochim. Cosmochim. Acta* **1995**, *59*(17), 3655–3661.

(37) Sherman, D. M.; Randall, S. R. *Geochim. Cosmochim. Acta* **2003**, *67*(22), 4223–4230.

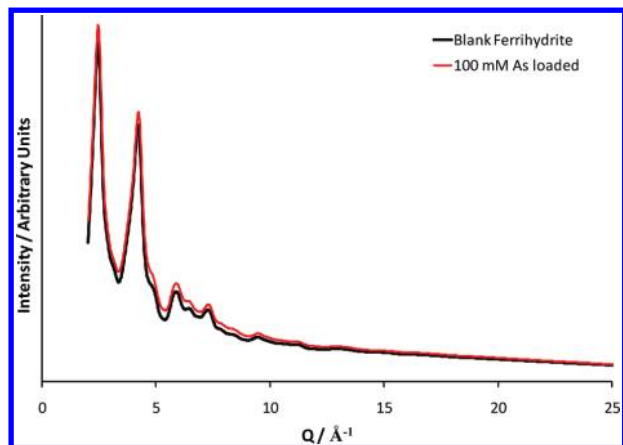


Figure 1. High energy X-ray diffraction pattern 2-line ferrihydrite (red) and 2-line ferrihydrite exposed to 100 mM arsenate solution (black).

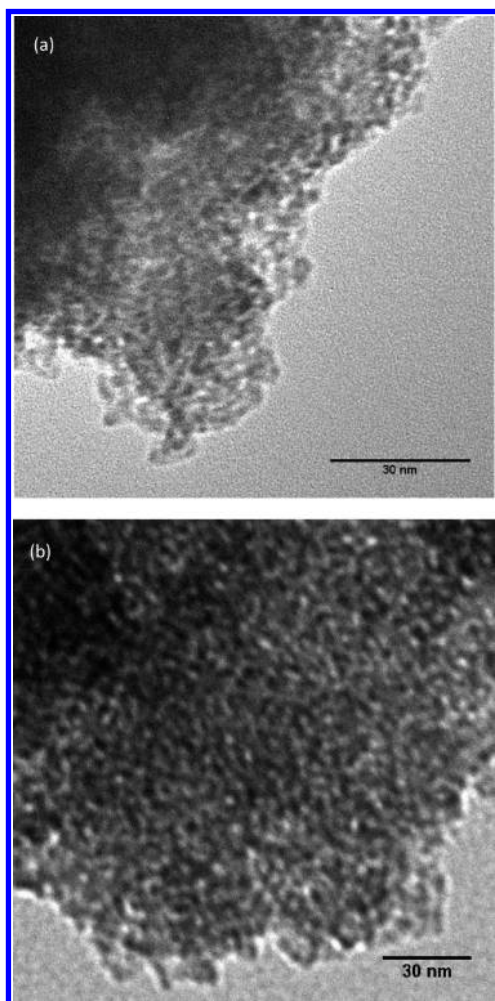


Figure 2. TEM micrograph of an aggregate of (a) ~ 2 nm 2-line ferrihydrite particles and (b) ~ 2 nm 2-line ferrihydrite particles exposed to 100 mM arsenate solution. Particles in the micrograph appear homogeneous and approximately 2 nm in size.

morphological changes or large scale precipitates formed because of exposure.

Powder diffraction experiments were carried out at station 11-ID-B at the Advanced Photon Source (APS), Argonne National Laboratory, using monochromatic X-rays of energy ~ 58 keV ($\lambda = 0.2128$ Å). Samples were loaded dry into a polyimide (Kapton) capillary. The scattered beam was

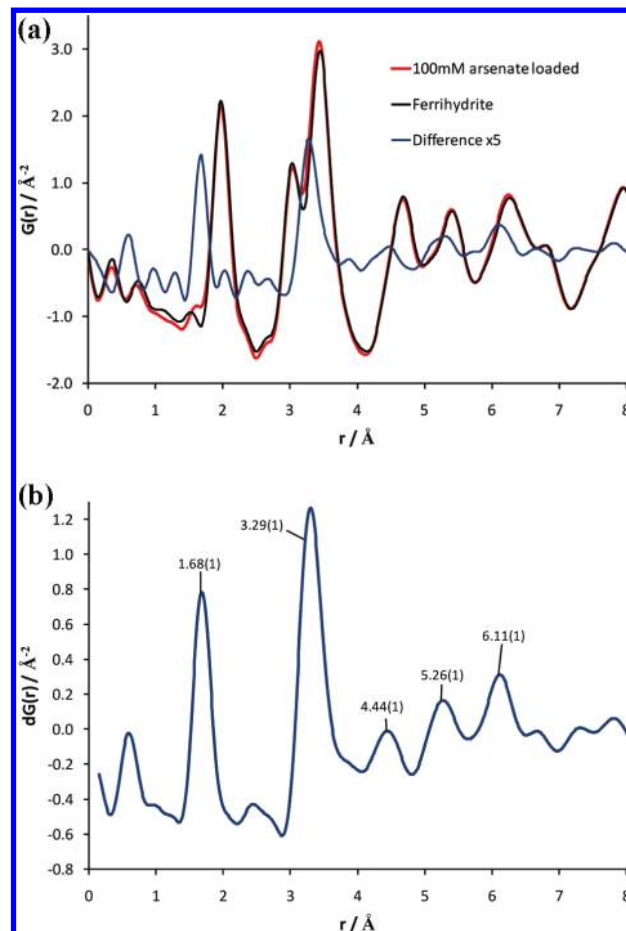


Figure 3. PDFs of (a) ferrihydrite (black), ferrihydrite exposed to 100 mM arsenate solution (red) and 5 \times the difference between them (blue), (b) The d-PDF of arsenate adsorbed on 2-line ferrihydrite r -averaged over normalization ripples.

collected on a Perkin-Elmer amorphous silicon detector, greatly reducing the required collection time, making the detection and interpretation of weak signals possible.^{38–40} The data conversion from 2D to 1D was carried out using the program fit2D.^{41,42} PDFs were generated by Fourier transformation of the total structure function, $S(Q)$, with a Q_{\max} of 24 \AA^{-1} , using the program PDFgetX2,⁴³ corrected for background scattering, Compton scattering and oblique incidence as described previously.³⁸ The d-PDFs were obtained by subtraction of the control PDF (2-line ferrihydrite with no surface loading) from the PDF of the loaded sample using Microsoft Excel. The control was multiplied by an appropriate constant to ensure the scale of each PDF was the same. Cluster analysis was carried out using the program DISCUS;⁴⁴ d-PDFs were calculated using distances

(38) Chupas, P. J.; Qiu, X.; Hanson, J. C.; Lee, P. L.; Gery, C. P.; Billinge, S. J. L. *J. Appl. Crystallogr.* **2003**, *36*(6), 1342–1347.

(39) Lee, J. H.; Aydiner, C. C.; Almer, J.; Bernier, J.; Chapman, K. W.; Chupas, P. J.; Haefner, D.; Kump, K.; Lee, P. L.; Liener, U.; Miceli, A.; Vera, G. *J. Synchrotron Radiat.* **2008**, *15*, 477–488.

(40) Chupas, P. J.; Chapman, K. W.; Lee, P. L. *J. Appl. Crystallogr.* **2007**, *40*, 463–470.

(41) Hammersley, A. P.; Svenson, S. O.; Hanfland, M.; Hauserman, D. *High Pressure Res.* **1996**, *14*(4–6), 235–248.

(42) Hammersley, A. P. *Fit2D V12.077 Reference Manual V. 3.1*; ESRF Internal Report, ESRF98HA01T; European Synchrotron Radiation Facility: Grenoble, France, 1998.

(43) Qui, X.; Thompson, J. W.; Billinge, S. J. L. *J. Appl. Crystallogr.* **2004**, *37*, 678.

(44) Proffen, T.; Neder, R. B. *J. Appl. Crystallogr.* **1997**, *30*, 171–175.

from Sherman and Randall³⁷ in a single unit cell of arbitrary dimensions, so that only correlations arising from within the cluster were calculated. Interatomic distances of interest were quantified by fitting the peak with a Gaussian function.

Results and Discussion

Figure 1 compares the XRD patterns of ferrihydrite and ferrihydrite exposed to a 100 mM arsenate solution; Figure 2 shows the corresponding transmission electron micrographs. Such high concentrations were used to ensure a high arsenate surface coverage, making the conditions as favorable as possible for the d-PDF experiment. One worry with using such a highly concentrated arsenate solution is the possibility of forming a precipitate. The XRD pattern exhibits no additional peaks, and the micrograph shows no additional phases for the 100 mM arsenate exposed sample. Taken together, the

results preclude the presence of a significant amount of a secondary phase.

Figure 3 shows the d-PDF for the sample exposed to a 100 mM arsenate solution. The first two peaks in Figure 3b at 1.68 Å and 3.29 Å match well with the peaks observed using EXAFS^{33,37} and are assigned as As–O and As–Fe correlations, respectively. Figure 4 shows the d-PDFs calculated from the clusters attained by Sherman and Randall³⁷ compared with the experimental d-PDFs, considering only the first two peaks. In each case, the experimental As–O correlation overlaps with the calculated peak; this distance is so similar in each cluster that it cannot be used as diagnostic of binding mechanism. EXAFS studies distinguish between the binding mechanisms using the As–Fe correlation distance. This is the case with d-PDF: Figure 4a compares the experimental d-PDF with that calculated from the bidentate binuclear model, the two As–Fe peaks overlap very well.

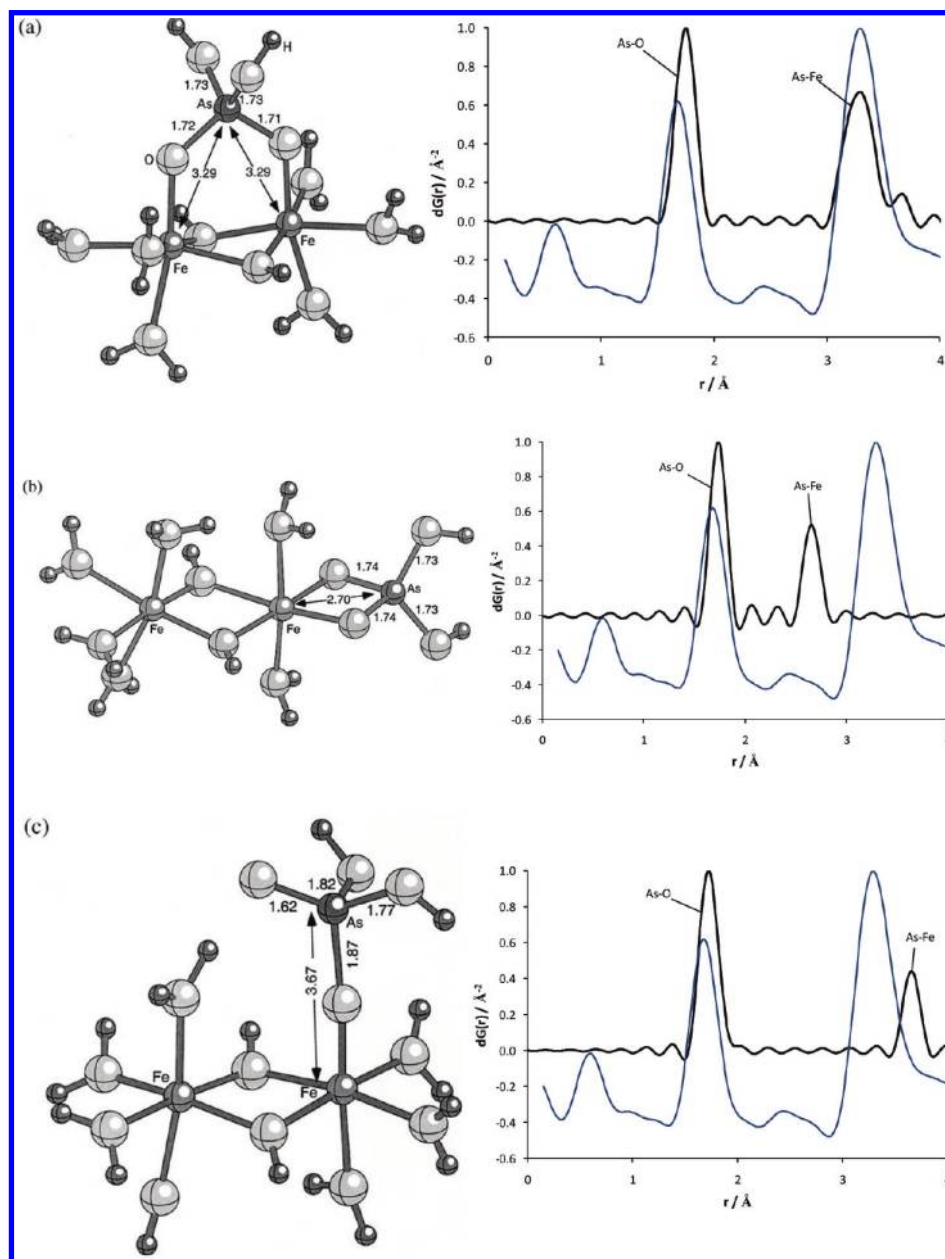


Figure 4. (a) Calculated d-PDF for a bidentate binuclear cluster, (b) calculated d-PDF for a bidentate mononuclear cluster, (c) calculated d-PDF for a monodentate cluster. In each the black line is the calculated d-PDF, the blue line the experimental data. Clusters are adapted from Sherman and Randall.³⁷

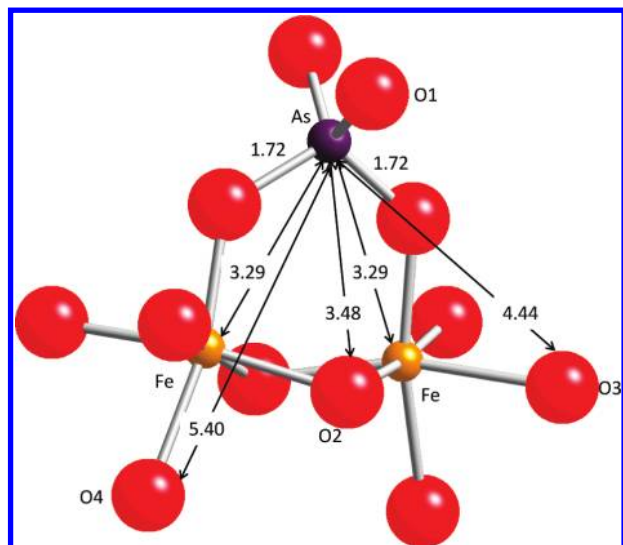


Figure 5. Redrawn bidentate binuclear cluster from Sherman and Randall,³⁷ with further bond distances added. All distances are in Å.

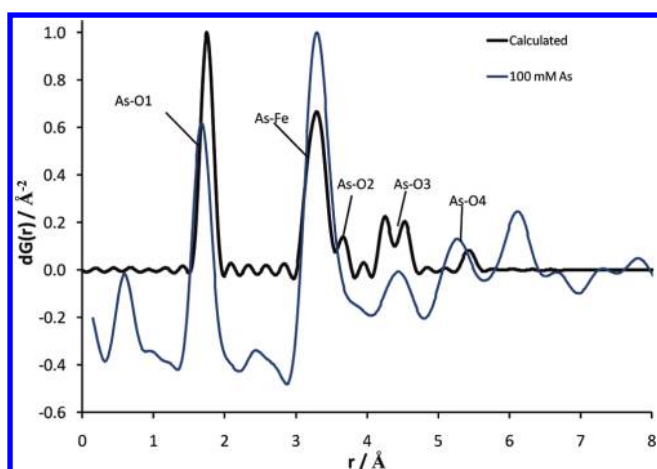


Figure 6. Comparison between the d-PDF calculated from the cluster in Sherman and Randall³⁷ (black) and the experimental d-PDF (blue) to higher r .

Figure 4b shows the calculated d-PDF for the bidentate mononuclear cluster; the As–Fe distance is much shorter than observed. Likewise, the monodentate As–Fe distance, Figure 4c, is longer than observed. This leads to the conclusion that the predominant binding mechanism in these samples is bidentate binuclear, confirming previous results derived from EXAFS spectroscopy.^{33,37}

The sharpness of the peak at 3.29 Å indicates that a monodentate model is unlikely. The As–O–Fe bonds in the monodentate system would have a large degree of freedom, leading to a large thermal factor and a broadening of this peak. It should be noted, however, that these experiments were carried out on dry samples. We surmise that significant hydration of the surface could lead to an equilibrium between bidentate binuclear and monodentate, or even more prevalent monodentate speciation as suggested in a recent study.⁴⁵

Further correlations in the d-PDF are observed at higher r , Figure 3. These are represented in Figure 5, a reproduction of

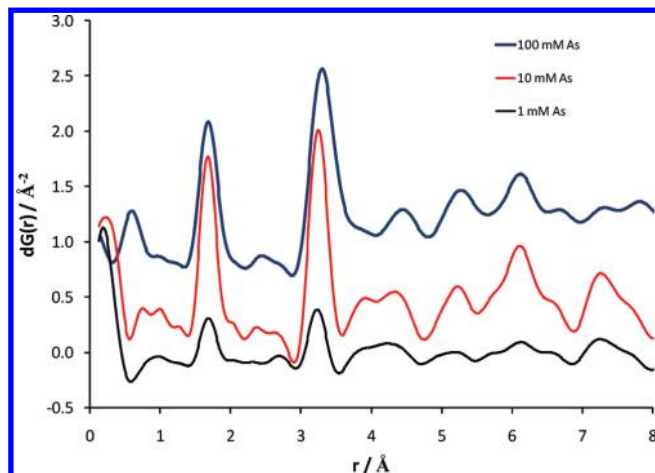


Figure 7. Comparison of d-PDFs obtained for samples exposed to different arsenate concentrations: 100 mM (blue), 10 mM (red), and 1 mM (black). Each is r -averaged over normalization ripples.

the bidentate binuclear cluster calculated by Sherman and Randall. The next correlation after As–Fe would be As–O2 (2 equivalent oxygens); this is not readily observed as it overlaps with the larger As–Fe peak. The next peak observed is at 4.44 Å, corresponding to the As–O(3) correlation (4 equivalent oxygens). The distances calculated by Sherman and Randall range from 4.181 Å to 4.581 Å; the experimental peak is not as sharp as the first two peaks, suggesting there may be a range of distances, but perhaps not as wide of a range obtained in the DFT calculations performed by Sherman and Randall. The next correlation at 5.26 Å corresponds to As–O4 (2 equivalent oxygens). Figure 6 compares the experimentally derived d-PDF with one calculated from the bidentate binuclear cluster of Sherman and Randall. Only peaks arising from As containing correlations are considered; the two agree very well. The splitting of the peaks As–O2 and As–O4 are due to the range of bond lengths in the cluster, as discussed above. The sharper experimental peaks suggest this is not the case in reality.

The assignment of the final peak at 6.11 Å is not as straightforward; the cluster calculated by Sherman and Randall does not extend to these distances. The two best candidates are an As to second Fe distance or the correlation between two arsenic atoms in adjacent clusters on the surface. Figure 7 shows d-PDFs of samples produced with arsenate solutions of different concentration used in the sorption process. The signal-to-noise decreases as loading is decreased. No signal was observed from samples exposed to a 0.1 mM arsenate solution (not shown). The peak at 6.11 Å is present in each PDF and does not decrease in intensity with respect to the other peaks as the arsenate concentration is decreased. If this peak were due to correlations between As–As clusters on the surface of the particle, this peak would diminish with decreasing concentration of arsenate solution as the surface concentration decreases; since this is not the case, it is believed that the best candidate for this peak is an As–2nd Fe. Density functional theory (DFT) calculations were carried out on extended clusters, but this proved unsuccessful as the torsional angle is free to rotate in this cluster; a small change in this angle has a large effect on the distances between atoms at larger distances. The lack of a surface model for ferrihydrite makes the assignment of higher distance correla-

(45) Loring, J. S.; Sandstrom, M. H.; Noren, K.; Persson, P. *Chem.—Eur. J.* **2009**, *15*, 5063–5072.

tions problematic. Improved theoretical representation of the ferrihydrite surface must be sought if quantitatively accurate longer range correlations are to be obtained from such simulations.

The experimental observation that d-PDF derived intensity is obtained from these samples is evidence for inner sphere coordination, that is, arsenate bound directly to the surface, rather than through a layer of intervening water. Signals associated with arsenate bound to water would be very weak, and it is unlikely that such a signal would be resolved over the background. This, of course, does not preclude the presence of outer sphere coordination along with inner sphere, as previously suggested.³⁴

Conclusions

Differential pair distribution function (d-PDF) analyses were carried out on ferrihydrite nanoparticles loaded with arsenate oxyanions. At high arsenate surface loading, correlations were observed due to As–O and As–Fe at 1.68 and 3.29 Å, respectively, agreeing very well with the previous EXAFS studies, confirming a bidentate binuclear binding mechanism. Further correlations, not observed by EXAFS, were present corresponding to further As–O distances. One further correlation is observed at 6.11 Å, ascribed to an As–2nd Fe distance.

Synthetic and experimental protocols introduced in this study represent a potentially powerful technique for the investigation of surface binding mechanisms on nanoparticles. Although there are limitations (a reasonably high level of surface speciation is required), d-PDF provides complementary information to EXAFS for systems with high surface areas. Improvements to existing data collection, such as the next generation of high energy, high flux synchrotrons and energy discriminating detectors could make this technique routine even when analyzing relatively low concentrations of adsorbed species.

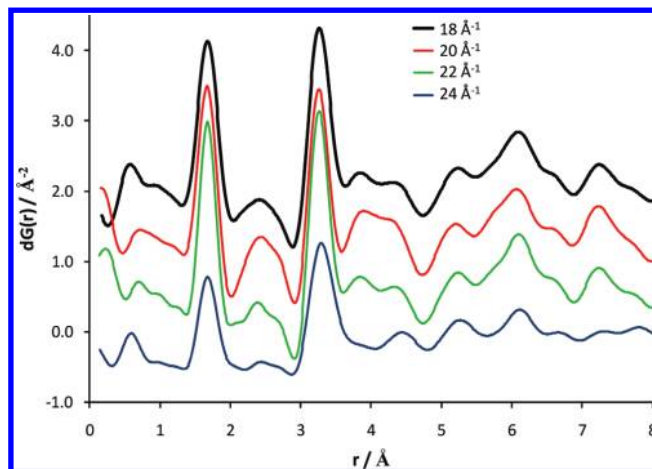


Figure A1. Comparison of differential PDFs of 100 mM samples calculated using different values of Q_{\max} in the Fourier transform.

Figure A1 shows a comparison of 100 mM As d-PDFs Fourier transformed using different values of Q_{\max} . The peaks corresponding to atomic correlations remain at the same value of r , while the noise peaks change position with change in Q_{\max} used.

Acknowledgment. We thank David Sherman for information regarding the clusters used in his paper with Simon Randall in 2003. We acknowledge financial support provided by the National Science Foundation (NSF) through Collaborative Research in Chemistry (CRC), Grant CHE0714183. D.R.S. acknowledges support from the NSF (CHE0714121). Work done at Argonne and use of the Advanced Photon Source was supported by the U. S. Department of Energy, Office of Science, Office of Basic Energy Sciences, under Contract No. DE-AC02-06CH11357.